Int. J. Heat Mass Transfer. Vol. 14, pp. 963–973. Pergamon Press 1971. Printed in Great Britain

TOTAL EMISSIVITY OF HOT WATER VAPOR—II.* SEMI-EMPIRICAL CHARTS DEDUCED FROM LONG-PATH SPECTRAL DATA

FREDERICK P. BOYNTON
and
CLAUS B. LUDWIG
Convair Division of General Dynamics, Space Science Laboratory, San Diego, California 92112, U.S.A.

(*Received* 19 *April* 1969)

Abstract—Recently measured band-model parameters for water vapor at high temperatures are used, together with other theoretical and experimental spectroscopic data, to develop the total emissivity of hot water vapor at various conditions for temperatures between 600° and 2500°K. The results are presented in chart form. At low temperatures, emissivities obtained from these charts agree satisfactorily with those obtained from Hottel's charts. At higher temperatures, where Hottel's charts rely heavily on graphical extrapolations, significant disagreement is found, and the new emissivities are in better agreement with theoretical predictions. Agreement of the new emissivities with the data upon which Hottel based his correlation is satisfactory for conditions where Hottel places high confidence in the data.

NOMENCLATURE

- a, ratio of line width to line spacing (γ/d);
- B_λ, Planck function;
- C_w, pressure-composition correction factor for H_20;
- d, line spacing;
- D, factor containing spectral dependence of a;
- k, absorption coefficient;
- l, path length;
- p, partial pressure;
- P_T, total pressure;
- T, absolute temperature;
- x, mole fraction;
- γ, line spacing;
- γ^* resonant dipole contribution to Γ;
- γ_j, non-resonant contribution of species j to γ;
- Γ, factor containing pressure and composition dependence of a;
- ϵ, emissivity;
- σ, Stefan–Boltzmann constant.

INTRODUCTION

HEAT transferred by radiation from a hot gas at uniform temperature, pressure, and composition is determined by its temperature and total emissivity. Water vapor is a prominent constituent of the combustion products of most common fuels, and considerable study has been given to its emissive properties, both spectral and total, since Schack [1] demonstrated the relation between infrared absorption and the total emissivity. A considerable body of total emissivity data were assembled in the 1920s and 1930s. These data showed that the total emissivity depends upon temperature, composition, pressure, and optical path length. Hottel and his coworkers reduced and correlated their own and other people's measurements over many years; these studies culminated in the preparation

* I. High pressure limit published in *Int. J. Heat Mass Transfer* **9**, 853–864 (1966).

of two charts [2], which can be used to obtain the total emissivity at a variety of conditions.

Hottel's charts are based upon a careful evaluation and correlation of experimental measurements. Total emissivities derived from these charts are entirely satisfactory for engineering predictions of heat transfer from homogeneous volumes of hot water vapor at conditions near those of the measurements. However, the charts also show estimates of the total emissivities based on extrapolation of the data to other conditions —primarily long paths, high temperatures, and pressures other than atmospheric—and in these situations the values derived from the charts are less accurate. Some current applications, such as radiative heat transfer from rocket combustion gases, involve hot water vapor at conditions where the chart values are extrapolated over a considerable distance from the measured data.

Penner [3, 4], Edwards [5] and their coworkers have performed a number of studies in which they interpreted Hottel's charts and band absorption data from various sources in terms of fundamental spectroscopic theory, which could be used to extrapolate the total emissivities to conditions different from those measured. A very important result of these studies is the demonstration that the statistical band model of Mayer [6] and Goody [7] describes the emissivity of hot water vapor. The statistical model gives the average spectral emissivity within a wavelength interval large enough to include many spectral lines. The line positions and strengths within the interval are described by distribution functions, rather than by detailed calculation. For a random distribution of line positions and an exponential distribution of line strengths, the averaged spectral emissivity for a gas in which collision broadening predominates (Lorentz line shape) is

$$\epsilon_\lambda = 1 - \exp[-\bar{k}_\lambda pl/(1 + \bar{k}_\lambda pl/4a_\lambda)^{\frac{1}{2}}] \quad (1)$$

where $\bar{k}_\lambda$ is the average absorption coefficient in the interval, p the partial pressure of the emitting species, l the path length, and a_λ the average ratio of line width to line spacing in the interval. Other functional expressions result from other distribution functions, but the effect of varying the intensity distribution on the path length dependence of ϵ_λ (the curve of growth) is not great. Penner, in particular, has used equation (1) with several different models for $\bar{k}_\lambda$ and a_λ to predict total emissivities which are in fair agreement with Hottel's charts.

Our laboratory has conducted a number of studies of hot water vapor emission, motivated by the need to predict infrared emission and radiative heating from rocket exhaust plumes. A set of empirically determined average spectral absorption coefficients [8] was derived from measurements of spectral emissivities performed here and elsewhere. These absorption coefficients were used to compute the total emissivities of hot water vapor at moderately high pressures [9]. This value of the emissivity represents an upper bound to the emissivity at lower pressures, and can be used for conservative estimates of radiative heating at conditions outside the range of Hottel's collected measurements. Predicted total emissivities at lower pressures [10] were derived from absorption coefficients by the use of a band-averaged (wavelength-independent) fine structure term, a_λ; good agreement was shown with Hottel's data (though the agreement was less satisfactory in the extrapolated region of the chart) and with band-absorption data obtained by Edwards *et al.* [5], and by Burch and Gryvnak [11].

More recently we have measured the spectral emission and absorption of hot water vapor at high temperature and long path lengths. These measurements were made in H_2–O_2 flames at temperatures between approximately 1200°K, and 3000°K, atmospheric pressure, and path lengths between 5 and 20 ft. The spectral interval covered was approximately 1·08–8·7 μ, which includes the spectral bands responsible for over 90 per cent of the emission at these conditions. These measurements have considerably extended the range of conditions for which H_2O emission data are available.

These new data, together with our own previous data and others available from several other sources, have been reduced [12–14] to obtain the parameters $\bar{k}_\lambda$ and a_λ of equation (1). The absorption coefficients are not greatly different from those previously reported [8], and the effect of the changes on our previously computed high-pressure total emissivities [9] is small. However, the fine-structure parameter a_λ has now been determined over most of the spectral region important to emission from hot water vapor. In this paper we apply the values of $\bar{k}_\lambda$ and a_λ derived from these and other measurements to compute the total emissivity at various conditions, and present the results in chart form.

DATA REDUCTION AND EMISSIVITY COMPUTATION

The total emissivities presented subsequently depend substantially on our own data at temperatures above 1000–1200°K, and on others' data at lower temperatures. Our apparatus and data reduction procedure have been discussed in detail elsewhere [12, 13], so we merely review them briefly here. The flame is produced by burning H_2 and O_2 at various (lean) equivalence ratios in a long multiple-slot strip burner. Data taken in absorption and emission are reduced by well-known procedures [15] to obtain the flame temperature and spectral emissivity. The reduced data are averaged over 25 cm^{-1} intervals and plotted together with other available measurements as reduced curves of growth of the linear form

$$\{pl/\ln[1/(1-\varepsilon_\lambda)]\}^2 = \bar{k}_\lambda^{-2} + (4a_\lambda\bar{k}_\lambda)^{-1}\, pl. \quad (2)$$

The value of $\bar{k}_\lambda$ is determined from the intercept of the LHS plotted vs. pl; the value of a_λ is determined from $\bar{k}_\lambda$ and the slope of the line. In our data, p is taken from a calculation of equilibrium composition at the measured flame temperature.

In a flame, temperature and composition cannot be independently varied over the entire range one would wish. Our measurements at a given temperature do not account for the effect of composition on the emissivity. This effect occurs through the fine structure parameter a_λ because collisions of the water molecule with different other molecules produce different amounts of broadening of the water lines. The principal broadening species present in our measurements were H_2O and O_2. In most applications, one needs to know not only the broadening effects of these species, but also those of others such as N_2, H_2, CO and CO_2. We have not measured these effects (though some of the data included in our collection were obtained with other broadeners). We must therefore introduce a model for the effect of composition of a_λ in order to extrapolate our values to other compositions.

The fine-structure parameter $a_\lambda = \gamma/d$ is the ratio of line width γ to the line spacing d. In any spectrum, d is a characteristic of the emitting molecule at a particular temperature and wavelength, while γ (for collision broadening) depends on the collision partner, the temperature, the pressure, and the particular lines being broadened. Computations of the line broadening in H_2O by Benedict and Kaplan [16] show that the dependence of γ on the rotational quantum numbers involved in particular lines is similar for broadening by H_2O, O_2 and N_2. We therefore assume that the ratios of the contributions to γ by different collision partners are independent of wavelength, and split a_λ into a factor Γ, which contains the effects of composition and pressure, and a factor $1/D$ which contains the spectral dependence. We express Γ as follows:

$$\Gamma = \sum_j \gamma_{j(\mathrm{STP})}\, p_j \left(\frac{273}{T}\right)^{\frac{1}{2}} + \gamma^*_{(\mathrm{STP})}\, p_{H_2O} \left(\frac{273}{T}\right), \quad (3)$$

where γ_j is the line width per unit partial pressure due to non-resonant collisions with the jth species, and γ^* is the line width per unit partial pressure due to resonant dipole–dipole collisions between H_2O molecules. The temperature dependencies (at constant pressure) result from assuming optical collision diameters independent of collision energy. The values of γ_j and

Table 1. Line widths per unit partial pressure for various broadening species

γ^*	0.44
γ_{H_2O}	(0.09)
γ_{N_2}	0·09
γ_{O_2}	0·04
γ_{H_2}	(0·05)
γ_{CO_2}	0·12
γ_{CO}	(0·10)

γ^* are given in Table 1; they rely heavily on the computations of Benedict and Kaplan except for the values in parentheses, which are estimates. With Γ calculated in this fashion, we have derived wavelength-dependent values of $1/D$ from the previously obtained values of a_λ.

The total emissivity at a particular condition is then developed as follows: Spectral emissivities in the region covered by our measurements and for which reliable values of $1/D$ could be obtained ($8{\cdot}7 > \lambda > 1{\cdot}33\,\mu$) are calculated from the derived values of $\bar{k}_\lambda$ and $1/D$ and the computed value of Γ for the particular temperature, pressure, and composition. Spectral emissivities at $\lambda > 8{\cdot}7$ are computed using a previously developed analytical expression [17] for the absorption coefficient of the pure rotation band of H_2O; spectral emissivities at $1{\cdot}33 > \lambda \geqslant 1{\cdot}0\,\mu$ are computed from the measured absorption coefficients. In both these regions, the value of $1/D$ is approximated by a sine function expression which allows lines to be closely packed in the band wings and less densely packed in the band centers, a behavior which follows the trend of the measured values and is also expected from theoretical considerations. The total emissivity is then

$$\varepsilon = \int_{\lambda_{min}}^{\infty} B_\lambda\, \varepsilon_\lambda\, d\lambda/\sigma T^4, \qquad (4)$$

where B_λ is the Planck function. For the conditions reported here, λ_{min} is about 1 μ, since shorter wavelengths contribute very little to the emission.

The errors in total emissivities calculated from this procedure depend on temperature and path length. The contribution from wavelengths between 8·7 and 1·3 μ for gas compositions close to those measured is estimated to be in error by less than ± 5 per cent. At different compositions, the error could be larger because of the necessity to assume a model for γ. Examination of previously computed [10] changes in the total emissivity for assumed changes in broadening coefficient shows that the maximum error in ε for reasonable variations in γ is about 10 per cent. The error associated with the contribution from shorter wavelengths is about 10 per cent of the path lengths listed; this error does not depend much on composition, since the fine structure effects are small under the conditions where this region contributes much emission. Somewhat larger errors are expected to be associated with the contribution

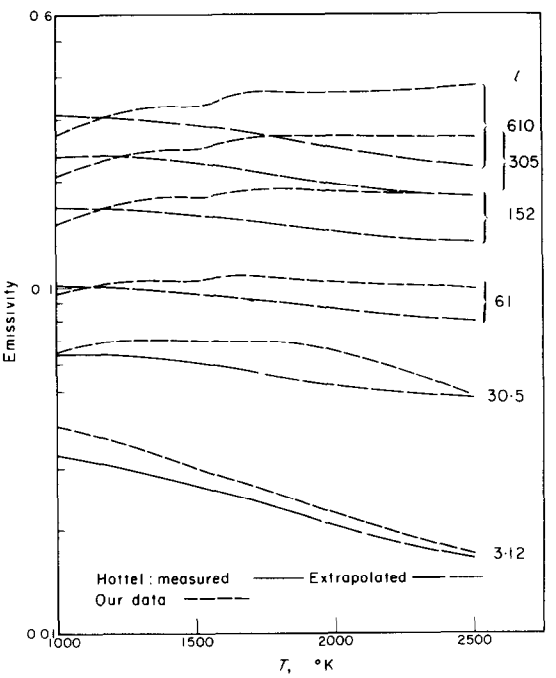

FIG. 1. Comparison of reconstituted experimental data with values from Hottel's charts ($P_T = 1$ atm).

from longer wavelengths; we estimate the errors to be ±20–30 per cent. These different errors in different wavelength regions contribute to the total error in proportion to the contributions of the respective spectral regions to the total emission, and also probably compensate each other to a degree. We believe that over most of the conditions reported an error of ±10 per cent is a reasonable estimate; at the lower temperatures and shorter paths, the error is probably ±15 per cent.

We have compared our measurements with values obtained from Hottel's charts. The comparison cannot be performed directly, because our spectral measurements did not cover all the wavelengths which contribute to water vapor emission at our experimental conditions. For this reason, we have "reconstituted" the total emissivities for our experimental conditions from our derived data and added the contributions of other spectral regions (which are small) according to the procedure described above. (The spectral emissivities thus recomputed are in excellent agreement with those measured, showing the consistency of the derived $\bar{k}_\lambda$s and a_λs.) The comparison is shown in Fig. 1, in which our reconstituted measurements are shown as dotted lines and Hottel's values are shown as solid or dashed lines. At temperatures below 1500°K, where Hottel's charts are closely related to measured data, the values agree to within the combined estimated errors, although the trend of the curves is somewhat different. At higher temperatures, however, our values lie considerably above Hottel's values, which are extrapolated. This large difference is much greater than the effect of gas composition (Hottel's data are derived from measurements in which N_2 and H_2O were the principal line broadeners) or of any error in our measurements or subsequent operations, and shows the need for a revision of the charts in this area. It is interesting to note that similar differences were shown in our predictions [10] and in the theoretical predictions of Penner and Varanasi [4].

RESULTS AND COMPARISONS

We have prepared charts, similar in concept to Hottel's, to show the total emissivity of hot water vapor at various conditions. In preparing these charts, we have attempted to keep the number of independent variables as small as possible, as Hottel did in his presentation. However, the wide temperature range covered in our charts affects the pressure/composition dependence to a degree which should not be ignored. Like Hottel, we show the total emissivity as a function of temperature for various optical paths pl for an infinitely dilute mixture of water vapor and other gases at a total pressure $P_T = 1$ atm; we also show a chart which is used

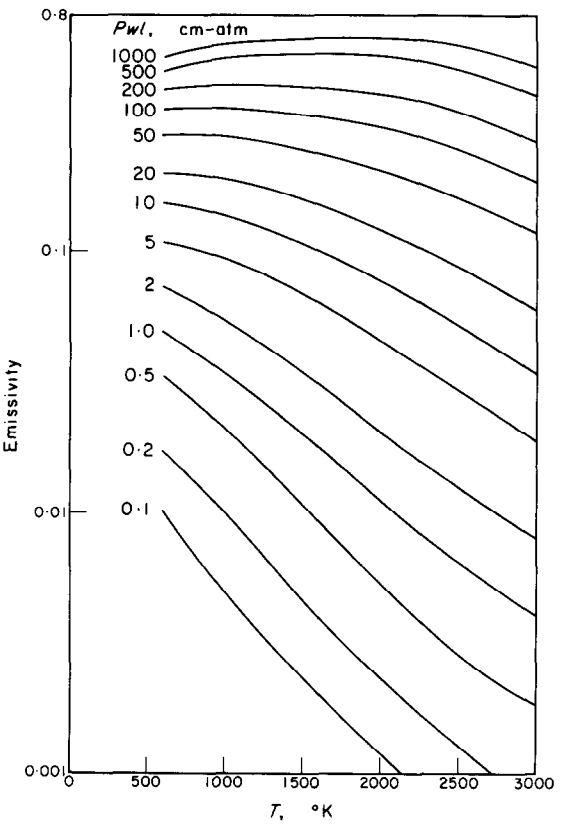

FIG. 2. Emissivities at infinite dilution ($p = 0$, $P_T = 1$) from our data.

to convert emissivities read from the first chart to other pressures and compositions.

The emissivity of hot water at $p = 0$, and $P_T = 1$ atm is shown in Fig. 2. In preparing this chart, we have assumed that $\gamma_{j(\mathrm{STP})} = 0{\cdot}09$. Emissivities read from this chart are thus correct if N_2 is the principal foreign gas. Inspection of the data shown in Table 1 indicates that for most practical applications, in which air or H_2 are the predominant foreign gases, the values should be reasonably accurate.

The correction chart, giving the quantity C_w by which $\varepsilon(p = 0, P_T = 1)$ is multiplied to obtain $\varepsilon(p, P_T)$, in Fig. 3. This chart is more complicated than Hottel's, since we have retained the temperature dependence of C_w. This temperature dependence is evident in the intermediate plots of Hottel and Egbert [18],

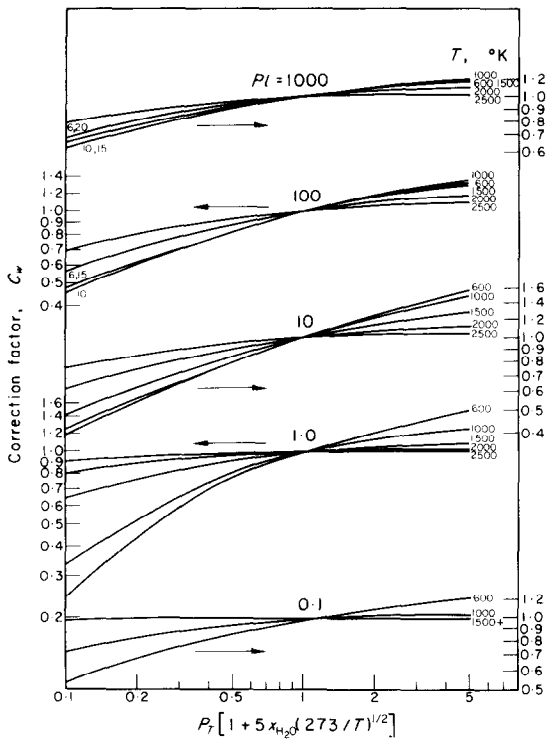

FIG. 3. Correction factor C_w as a function of the pressure parameter at different temperatures and optical depths.

but was omitted in their final chart in order to simplify the presentation. Since their work covers a smaller temperature range than ours (the data considered were taken between 400 and 1000°K), this omission was reasonable. In our results, the temperature dependence is significant. The plotted curves are C_w at various path lengths pl and temperatures as a function of pressure and water content, which according to the model of Γ and the γ_j and γ^* values of Table 1 can be expressed in combined form as $P_T[1 + 5x_{H_2O}(273/T)^{\frac{1}{2}}]$, where x_{H_2O} is the mole fraction of water vapor. This abscissa is different from Hottel's; we will comment on the difference subsequently. The chart shows that the correction factor, which shows the effect of fine structure, is most variable at low temperatures and least variable at high temperatures. At high temperatures there are many more lines in the spectrum of hot water vapor than at low temperatures, so the fine structure is effectively crowded out or filled up.

A brief review of the steps by which Hottel's charts were prepared is in order before we compare our total emissivities with his; full details can be found in the paper by Hottel and Egbert [18]. The charts were prepared by a series of graphical operations on a carefully reviewed set of data. The correction factor chart was prepared first, from data in which the water content was varied at constant path length and $P_T = 1$ atm. The temperature range of the data was 400–1000°K, and the effect of temperature on the curves was ignored. The resulting graph (Fig. 16 of [18]) was used to correct the measured emissivities at finite H_2O content to the infinitely dilute case, and Figs. 4–15 of [2] was then prepared.

The addition of the pressure dependence to the C_w plot was based upon a qualitative observation that "Dr. Fishenden found that absorption by pure steam at $\frac{1}{2}$ atm is equal to that by steam at a very low partial pressure mixed with N_2 to give a total pressure of 1 atm, so long as pl is the same in both experiments." ([18], p. 588). The extension to $P_T < 1$ atm

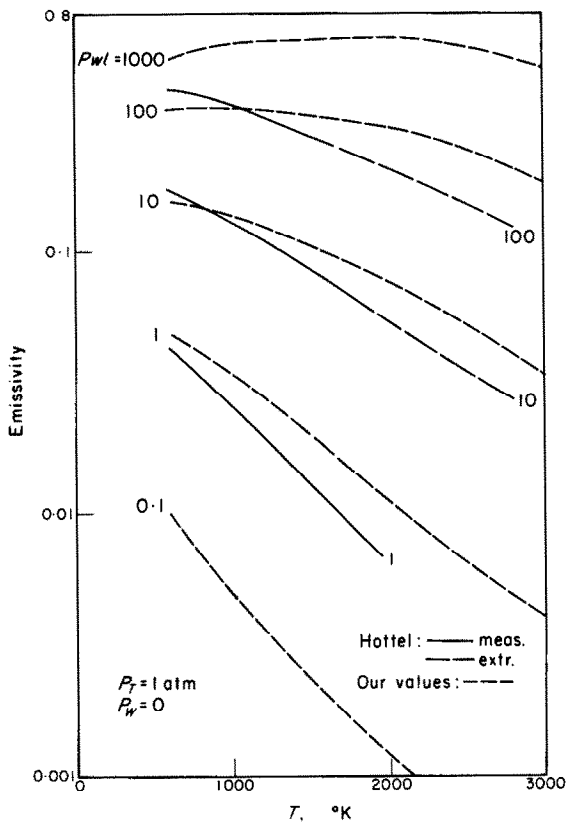

FIG. 4. Comparison of derived emissivities at infinite dilution with Hottel's values.

followed monochromatic absorption data obtained by von Bahr, and was to some extent arbitrary. Hottel has been careful to note that "although Figs. 4–16 of [2] is satisfactory for showing the separate effects of p and l on water vapor radiation at $P_T = 1$ atm, it must be considered a very rough approximation for estimating the effect of P_T when that differs appreciably from 1 atm" ([2], p. 84). We are thus not overly concerned that our pressure dependence is different from that reported by Hottel, though we would welcome consistent measurements made over a range of temperature at pressures different from one atm.

With these caveats in mind, we proceed to a comparison of our charts with Hottel's. A comparison of the basic charts is shown in Fig. 4. The two presentations agree to within the estimated errors in both at temperatures up to 1200°K at the longer paths. At higher temperatures, a systematic difference is encountered, with our curves lying consistently higher than those of Hottel. The trend of the curves is somewhat different at lower temperatures, but one should not make too much of these differences since the estimated error of our presentation is larger here.

A comparison of the final C_w charts would not have much significance, because of the considerably different methods and assumptions involved in their preparation. Neither chart is based on measurement of P_T effects on total emissivities. A more meaningful comparison is possible with the intermediate chart, Fig. 16 of [18]. This comparison is shown in Fig. 5. The heavy lines have been interpolated from Hottel and Egbert (the line at $pl = 1000$ was extrapolated); the shaded regions, which collapse nearly to a line at $pl = 1000$, are the limits of the composition effect which is specified by Fig. 3, as the temperature varies between 600° and 1000°K. This temperature region is close to that at which the measurements of Hottel and Egbert were taken. The agreement is satisfactory at the optical path lengths shown. Our temperature variations are also in the same direction as those shown in Fig. 15 of [18]. At short paths, our correlation shows a wide spread; Hottel shows few data at path lengths below 10 cm-atm, and the data exhibit more scatter than do those at longer paths. We therefore believe a comparison at shorter path length is not meaningful.

We have also compared total emissivities derived from our correlation with some of the data considered by Hottel and Egbert in preparing their charts. Figure 6 shows a comparison with the long-path data of Hottel and Mangelsdorf [19]. The agreement is quite satisfactory. Their data at short optical paths are believed to be incorrect because of considerable atmospheric absorption [19]; our correlation lies

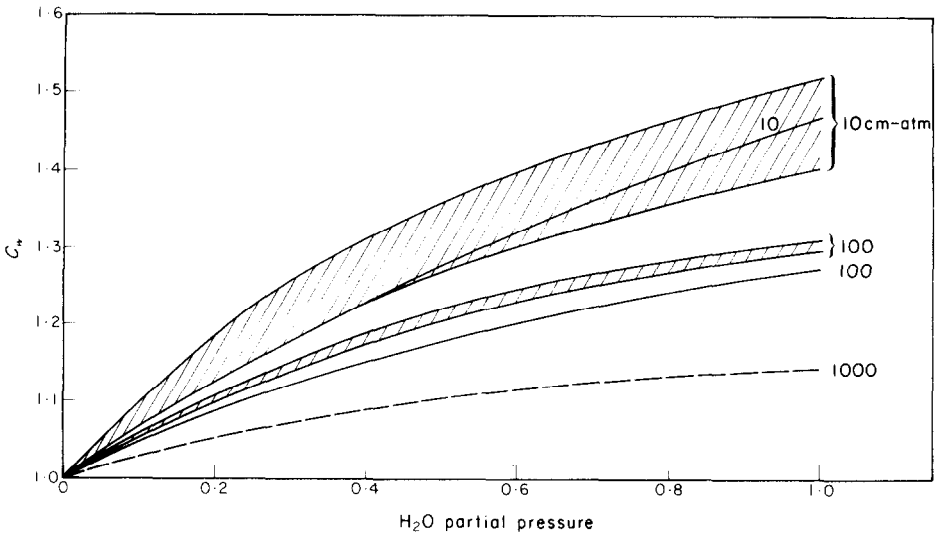

FIG. 5. Comparison of our correction factor C_w with Hottel and Egbert's curves ($P_T = 1$ atm).

considerably above their data for $\varepsilon \leqslant 0{\cdot}07$, as we would thus expect. A comparison with data plotted by Schmidt [20] is shown in Fig. 7; his data are for pure water vapor at a total pressure of 1 atm. The agreement is also satisfactory. Schmidt's basis for extrapolating his plots to temperatures above 1000°C, the assumption that the product of temperature and emissivity is constant, is approximately consistent with our deduced values at high temperatures and the optical depths of his experiments (but not at greater or lesser depths).

The most complete recent theoretical computation of water vapor emissivity is that of Penner and Varanasi [4]. In Fig. 8 we have compared their calculated values of the total emissivity of pure water vapor at $P_T = 1$ atm with those deduced by us. The agreement is excellent up to $pl = 152{\cdot}5$ cm-atm. Most of the difference at low temperatures at this path can be ascribed to different treatments of the rotational band. The dash-dotted line shows where their prediction would fall if they had used our rotational band expression instead of theirs.

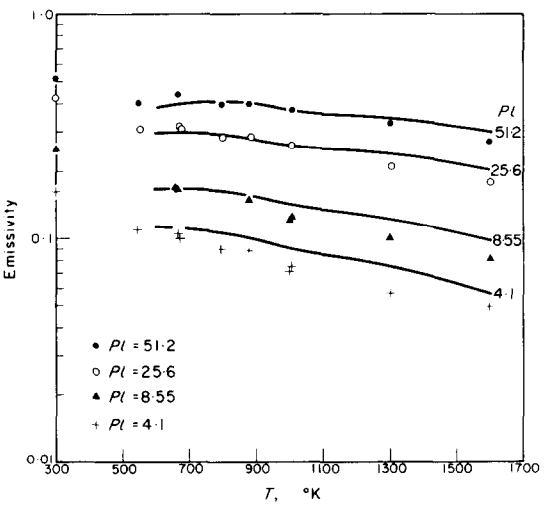

FIG. 6. Comparison of our derived emissivities with data from Hottel and Mangelsdorf.

(Our emissivities are still ~15 per cent below Hottel's at this condition. Recent measurements of the pure rotation spectrum by Penner and Varanasi [21, 22] have shown that our rotational band expression may underestimate the spectral

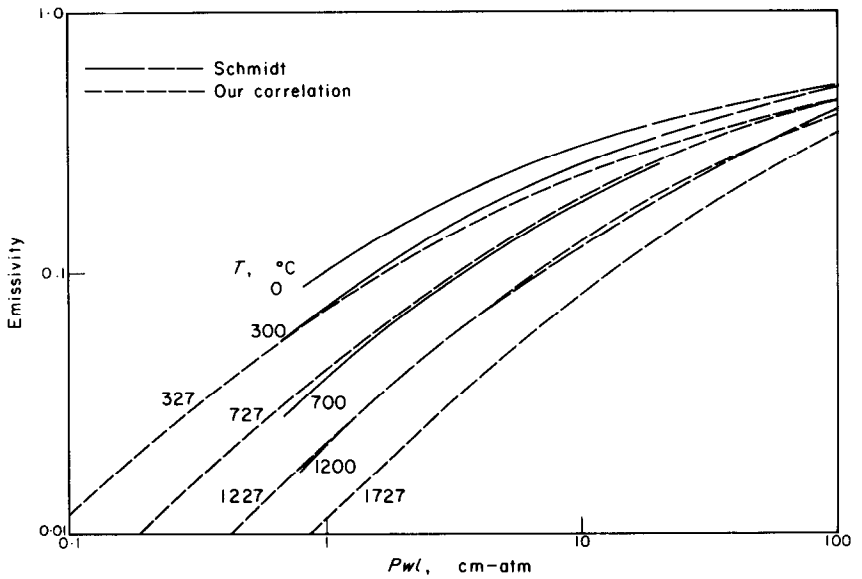

FIG. 7. Comparison of our derived emissivities with values presented by Schmidt.

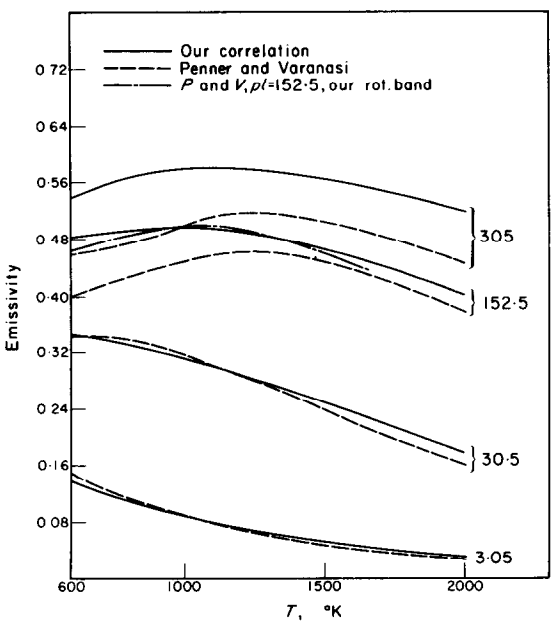

FIG. 8. Comparison of our derived emissivities with theoretical predictions of Penner and Varanasi.

emissivity between 10 and 15 μ. Accounting for this effect would bring both their predictions and ours closer to Hottel's data.) This difference, as well as the high-temperature differences at $pl = 305$ cm-atm, are due to the different wing contributions in our measured (or, for the rotational band, computed) spectra and in the harmonic oscillator-rigid rotator model used by Penner and Varanasi. At optical depths $\gtrsim 150$ cm-atm, the wings of the strong vibration–rotation fundamental bands begin to affect the change in total emissivity with increasing pl; the change is first apparent in the very intense rotational spectrum, and appears in the vibration-rotation bands also as pl increases. Although the agreement between their calculations and our semiempirical values is good at 1 atm, the pressure dependence at $P_T > 1$ atm is different; Penner and Varanasi [4] assumed that pure H_2O is fully pressure-broadened at 1 atm, while we expect some additional broadening at higher pressures.

REFERENCES

1. A. SCHACK, Mitteilungen der Wärmstelle Dusseldorf, Mitt. Nr. 55 (1924).
2. H. C. HOTTEL, Radiant heat transmission, *Heat Transmission*, edited by W. H. MCADAMS), 3rd edn., Chap. 4, pp. 55–125. McGraw-Hill, New York (1954).
3. S. S. PENNER, *Quantitative Molecular Spectroscopy and Gas Emissivities*, pp. 316–336. Addison–Wesley, Reading, Mass. (1959).
4. S. S. PENNER and P. VARANASI, Approximate band absorption and total emissivity calculations for H_2O, *J. Quant. Spectros. Radiat. Transfer* **5**, 215–227 (1965).
5. D. K. EDWARDS, B. J. FLORNES, L. K. GLASSEN and W. SUN, Correlation of absorption by water vapor at temperatures from 300°K to 1100°K, *Appl. Optics* **4**, 715–721 (1965).
6. H. MAYER, Los Alamos Scientific Laboratory Report LA–647 (1947).
7. R. M. GOODY, *The Physics of the Stratosphere*, pp. 161–163. Cambridge University Press, Cambridge (1954).
8. C. C. FERRISO, C. B. LUDWIG and A. THOMSON, Empirically determined infrared absorption coefficients of H_2O from 300 to 3000°K, *J. Quant. Spectros. Radiat. Transfer* **6**. 241–275 (1966).
9. C. C. FERRISO, C. B. LUDWIG and F. P. BOYNTON, Total emissivity of hot water vapor—I. High pressure limit, *Int. J. Heat Mass Transfer* **9**, 853–864 (1966).
10. C. B. LUDWIG and C. C. FERRISO, Predictions of total emissivity of nitrogen-broadened and self-broadened hot water vapor, *J. Quant. Spectros. Radiat. Transfer* **7**, 7–26 (1967).
11. D. E. BURCH and D. A. GRYVNAK, Infrared radiation emitted by hot gases and its transmission through synthetic atmospheres, Ford Motor Company, Aeronutronic Division, Report U–1929 (1962).
12. Study on exhaust plume radiation predictions. Final report, Contract NAS 8–11363. General Dynamics/Convair, Report GDC–DBE66–017 (Dec. 1966).
13. Study on exhaust plume radiation predictions. Progress report, Contract NAS 8–21082. General Dynamics/Convair Report GDC–DBE67–021 (Nov. 1967).
14. C. B. LUDWIG, Measurements of the curves-of-growth of hot water vapor, *Appl. Optics* **10**, No. 5 (1971).
15. S. SILVERMAN, The determination of flame temperatures by infrared radiation, *J. Opt. Soc. Am.* **39**, 275–277 (1949).
16. W. S. BENEDICT and L. D. KAPLAN, Calculation of line widths in H_2O–H_2O and H_2O–O_2 collisions, *J. Quant. Spectros. Radiat. Transfer* **4**, 453–469 (1964).
17. C. B. LUDWIG, C. C. FERRISO, W. MALKMUS and F. P. BOYNTON, High temperature spectra of the pure rotational band of H_2O, *J. Quant. Spectros. Radiat. Transfer* **5**, 697–714 (1965).
18. H. C. HOTTEL and V. C. SMITH, Radiation from non-luminous flames, *Trans. Am. Soc. Mech. Engrs* **57**, 463–470 (1942).
19. H. C. HOTTEL and H. G. MANGELSDORF, Heat transmission by radiation from non-luminous gases II. Experimental study of carbon dioxide and water vapor, *Trans. Am. Inst. Chem. Engrs* **31**, 517–549 (1935).
20. E. SCHMIDT, Messung der Gesamtstrahlung des Wasserdampfes bei Temperaturen bis 1000°C, *Forsch. Geb. Ingenieurw.* **3**, 57–70 (1932).
21. S. S. PENNER and P. VARANASI, Spectral absorption coefficients in the pure rotation spectrum of water vapor, *J. Quant. Spectrps. Radiat. Transfer* **8**, 1537–1539 (1968).
22. P. VARANASI, S. CHOW and S. S. PENNER, Absorption coefficient for water vapor in the 600–1000 cm^{-1} region, *J. Quant. Spectros. Radiat. Transfer* **8**, 1537–1539 (1968).

EMISSIVITÉ TOTALE DE LA VAPEUR D'EAU CHAUDE. II—TABLES SEMI-EMPIRIQUES DÉDUITES DES RÉSULTATS SUR UN SPECTRE ÉTENDU

Résumé—Des paramètres sur le modèle de bande récemment mesurés pour de la vapeur d'eau à hautes températures sont utilisés avec d'autres données spectroscopiques théoriques et experimentales pour déterminer l'émission totale de vapeur d'eau chaude pour diverses conditions de température comprise entre 600° et 2500°K. Les résultats sont présentés sous forme de tables. Aux basses températures, les émissivités obtenues dans ces tables sont en accord satisfaisant avec celles obtenues à partir des tables de Hottel. Aux températures plus élevées, où les tables de Hottel dépendent lourdement des extrapolations graphiques on trouve un écart significatif et les nouvelles émissivités sont en meilleur accord avec les prédictions théoriques. L'accord des nouvelles émissions avec les résultats sur lesquels sont basés les correlations de Hottel est satisfaisant pour des conditions où Hottel met une grande confiance dans les résultats.

DAS TOTALE EMISSIONSVERMÖGEN VON ÜBERHITZTEM WASSERDAMPF. II. SEMI-EMPIRISCHE DIAGRAMME, GEWONNEN AUS WEIT-WEG-SPEKTRAL-DATEN

Zusammenfassung—Um das totale Emissionsvermögen von überhitztem Wasserdampf zwischen 600 und 2500 K unter verschiedenen Bedingungen abzuleiten, werden kürzlich gemessene Band-Modell-Parameter für Wasserdampf bei hohen Temperaturen verwendet, zusammen mit anderen theoretischen und experimentellen spektroskopischen Daten. Die Ergebnisse werden in Form von Diagrammen geboten. Bei tiefen

Temperaturen stimmt das Emissionsvermögen aus diesen Diagrammen zufriedenstellend mit dem aus den Diagrammen von Hottel überein. Bei höheren Temperaturen, wo Hottels Diagramme sehr auf graphischen Extrapolationen beruhen, treten deutliche Unterschiede auf. Die neuen Zahlenwerte für das Emissionsvermögen stimmen besser mit theoretischen Voraussagen überein. Die Übereinstimmung der neueren Zahlenwerte mit den Daten, auf die Hottel seine Beziehungen stützt, ist zufriedenstellend bei Bedingungen, bei denen Hottel den Daten eine hohe Zuverlässigkeit zuschreibt.

ОБЩАЯ ИЗЛУЧАТЕЛЬНАЯ СПОСОБНОСТЬ ВОДЯНОГО ПАРА. ПОЛУЭМПИРИЧЕСКИЕ ДИАГРАММЫ, ПОСТРОЕННЫЕ НА ОСНОВЕ СПЕКТРАЛЬНЫХ ДАННЫХ ДЛЯ МОЛЕКУЛ С БОЛЬШОЙ ДЛИНОЙ ПРОБЕГА

Аннотация—Недавно измеренные параметры зонной модели для водяного пара при больших температурах используются вместе с другими теоретическими и экспериментальными спектроскопическими данными для вывода общей излучательной способности горячего водяного пара в разных условиях для диапазона температур от 600° до 2500°К. Результаты представлены в виде графиков. При низких температурах излучательная способность, полученная по этим графикам, удовлетворительно соответствует данным, полученным по графикам Хоттеля. При более высоких температурах, когда графики Хоттеля в основном основаны на графических экстраполяциях, обнаруживается значительное разногласие, и новые данные для излучательной способности больше соответствуют теоретическим расчётам. Соответствие новых данных для излучательной способности данным, на которых Хоттелб основывал свои соотношения, вполне удовлетворяет условиям, для которых Хоттель установил высокую достоверность.